Efficient and stable orbital-searching algorithm for the configuration interaction method and its application to quantum impurity problems

Chungwei Lin and Alexander A. Demkov

An efficient and stable orbital searching algorithm for the configuration interaction method and its application to quantum impurity problems

Chungwei Lin and Alexander A. Demkov[*]

Department of Physics, University of Texas at Austin

The configuration interaction (CI) method can be regarded as a generalization of the Hartree-Fock theory. The CI method includes multiple determinantal states to approximate the full many-body ground state, as opposed to just one in Hartree-Fock. In this work, we introduce an efficient and stable algorithm to obtain the optimal single-particle basis by formulating orbital searching in terms of a multi-variable minimization problem. The algorithm is iterative and is based on imaginary-time dynamics. It is numerically efficient as the Hessian (second derivative of the energy with respect to the orbital variables) is not required; It is also stable as a reasonable initial orbital choice is not necessary. The algorithm can deal with Hamiltonians with complex coefficients. We demonstrate the power of the proposed algorithm by applying it to impurity problems, with the most complicated one including multiple correlated orbitals and spin-orbit coupling. Energies and spectral functions are computed to demonstrate the convergence of the CI method.

I. INTRODUCTION

The configuration interaction (CI) method[1,2] is a straightforward generalization of the Hartree-Fock approximation. Instead of approximating the many-body state by a single determinantal state, the CI method systematically includes more determinantal states to better capture correlation effects. For some correlated systems, the inclusion of multi-determinantal states makes a qualitative difference and is of fundamental importance. Perhaps the simplest non-trivial example is the Kondo problem[3–5]. When introducing a local spin which couples to many uncorrelated bath electrons, the ground state becomes a spin singlet state, which intrinsically needs more than one determinantal state for a proper description. More generally, electron correlation is essential for phenomena such as superconductivity[6], metal insulator transition[7], and magnetic phase[8,9]. The CI method is widely used in quantum chemistry for small molecular systems[1,10]. Recently, first implemented by Zgid and Chan[11,12], the CI method has also been successfully applied to quantum impurity models[11–15]. In combination of dynamical mean field theory (DMFT)[16–20], the CI impurity solver can be used to study a lattice problem. Due to its manageable computational cost, the CI method is also used to study correlated time-dependent phenomena[21–24].

The most critical step of a CI calculation is to identify the optimal single-particle orbital basis. The traditional approach is to first formulate an equivalent multi-variable minimization problem, and iteratively search for the global minimum using the Newton-Raphson or related searching algorithms[1,25–28]. The convergence of these methods depends critically on the initial orbital basis. In particular, it may converge to a local minimum, instead of the global one[29]. Here we propose an imaginary-time-based orbital searching algorithm, which can largely avoid these shortcomings. In addition to being stable and efficient, it deals with complex coefficients within the same formalism, allowing us to take into account the electron correlation and spin-orbit coupling simultaneously. We believe our algorithm is

---

[*] E-mail: demkov@physics.utexas.edu

particularly useful for systems whose the electron correlation and spin-orbit coupling are of comparable strength, (e.g. $5d$ transition metals[30–32]), such that the perturbative approach is not appropriate.

The rest of the paper is organized as follows. In Section II, we briefly review the CI method and describe the proposed orbital searching algorithm. In Section III, we discuss several aspects of the algorithm, from general to technical. In Section IV, we provide a few examples to illustrate the efficiency of our method. The energy and spectral function are computed to show the convergence. A short conclusion is given in Section V. In the Appendix, we discuss the details of the orbital evolution in both real and imaginary time.

II. THE ORBITAL SEARCHING ALGORITHM
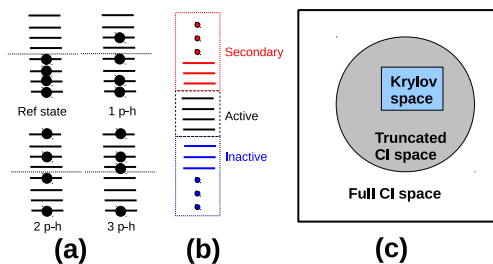
A. General CI schemes

FIG. 1: (Color online) Illustration of CI steps to systematically construct a small subspace. In a CI scheme, a state is classified by the number of particle-hole pairs with respect to a reference Fock state; and the orbitals by its occupation. (a) Based on the former, CI-n_{p-h} is to denote a subspace containing states of 0,1,...,n_{p-h} p-h pairs. CI-3 is illustrated. The dimension of CI-n_{p-h} scheme grows polynomially as the total orbital number increases. (b) Based on the latter, each kept Fock state has mostly empty secondary orbitals and mostly occupied inactive orbitals, but has no restriction on the active orbitals. Particularly for the CAS scheme, inactive and secondary orbitals are fully filled and empty respectively, so its dimension is independent of the total orbital number. (c) Out of the full CI space, the truncated subspace is chosen by some CI scheme. In the truncated CI space, one could further construct a Krylov space to get the ground state.

Once a complete set of single-particle orbitals (of dimension N_o) is specified, the complete N_e-body fermionic space can be constructed by listing all possible N_e occupied single-particle orbitals (Fock states). As the dimension of the full N_e-body fermionic space easily grows to a formidably large number when the system size increases, solving a many-body problem using exact diagonalization (ED) is only possible for small systems. The configuration interaction method[1,2,12,14] is based on the ED formalism, and its core is to identify a subspace, as small as possible, that can faithfully describe the true many-body ground state. To avoid a possible confusion, a following convention is adopted: in this paper, the "state" is referred to a *many-body* wave function; the "orbital" is referred to as a *single-particle* wave function that is used to build many-body states.

The CI method systematically classifies and selects states based on the following two criteria. First, the Fock states are classified according to the number of particle-hole (p-h) pairs with respect to a given reference state, where the chosen N_e orbitals are occupied. A CI scheme only keeps Fock states of a few p-h pairs; "CI-n_{p-h}" (n_{p-h} an integer) will be used to denote the CI scheme that includes states of 0,1,...,n_{p-h} p-h pairs. For example, the CI-3 scheme includes Fock states of 0,1,2, and 3 p-h pairs, and is also commonly referred to as CISDT (S: single; D: double; T:

triple) scheme [see Fig. 1(a)]. Second, the single-particle orbitals are classified based on their occupation. They are (1) inactive (mostly occupied); (2) secondary (mostly empty); or (3) active (no restriction) [see Fig. 1(b)]. Two types of truncation schemes based this criterion are introduced accordingly. In the "complete active space" (CAS) scheme, inactive orbitals are always occupied whereas secondary orbitals always empty. The notation $CAS(m, n_A)$ indicates filling m electrons in n_A active orbitals. In the "restricted active space" (RAS) scheme, the inactive orbitals are mostly occupied but are allowed to have a small number of holes; the secondary orbitals are mostly empty but are allowed to have a small number of particles; the active orbitals again have no constraints. The notation $RAS(n_I, -k; n_S, l)$ indicates allowing maximum k holes (we use minus sign to indicate the holes) in n_I inactive orbitals, and maximum l particles in n_S secondary orbitals. These classifications are discussed in details in Ref.[1], and in this paper we follow the same notations as in our previous work[14]. These two criteria can be, and frequently are combined to define the subspace in CI calculations.

The dimension of the CI-n_{p-h} and RAS schemes grows polynomially as the number of orbitals increases, which is significantly slower than the exponential growth of the full Fock space. The dimension of a CAS scheme, furthermore, depends *only* on the number of active orbitals, *not* on the total number of orbitals. Therefore, *if* the true ground state can be described in the CAS subspace, the CAS is the truncation scheme to use. Certainly there is no *a priori* reason to assume that a given CAS space, or any CI space, is sufficient, and practically one needs at least an additional calculation using a larger CI space to check the convergence. The main purpose of this paper is to introduce an orbital searching algorithm, which efficiently identifies the optimal orbital basis (the orbital basis which gives the lowest ground state energy) in the CAS space.

Once a CI subspace is specified, one could further use the power methods such as Lanczos[6] or Davidson algorithm[33] to obtain the many-body ground state. The power method in essence keeps only Krylov subspace spanned by

$$\{|\phi_0\rangle, H|\phi_0\rangle, H^2|\phi_0\rangle, ..., H^n|\phi_0\rangle\} \tag{1}$$

with H being the full Hamiltonian and $|\phi_0\rangle$ a random initial state. The hierarchy of choosing states out of the full space is summarized in Fig. 1(c)[34].

B. Variational principle and orbital degree of freedom

In view of variational principle, the CI approximation amounts to obtaining the best ground state in the truncated CI space. As mentioned previously, identifying the optimal orbital basis is the most critical step of a CI calculation. Following Ref.[25], we discuss the orbital degrees of freedom and formulate the orbital optimization in terms of a multi-variable minimization problem. For a complete orbital basis specified by $\{a^\dagger\}$, a general orbital rotation is given by

$$\begin{aligned} \tilde{a}_r^\dagger &= \exp(i\Lambda)a_r^\dagger \exp(-i\Lambda) \\ &= \sum_s a_s^\dagger \left[\exp(i\mathbf{\Lambda})\right]_{sr} = \sum_s a_s^\dagger X_{sr}, \end{aligned} \tag{2}$$

where $\Lambda = \sum_{rs} \Lambda_{rs} a_r^\dagger a_s$ is a Hermitian operator ($\Lambda_{rs} = \Lambda_{sr}^*$), and $\mathbf{X} = \exp(i\mathbf{\Lambda})$ is a unitary matrix. Equivalently, $\tilde{a}_r = \sum_s X_{rs}^\dagger a_s$ and $a_r = \sum_s X_{rs}\tilde{a}_s$. Note that the diagonal term Λ_{ii} only introduces a phase to the ith orbital, and without loss of generality we can take $\Lambda_{ii} = 0$[25].

Now we consider a many-body state in some CI space specified by Π

$$|\phi_0\rangle = \sum_{g\in\Pi} |g\rangle C_g^{(0)}, \tag{3}$$

with $|g\rangle$ being the Fock states built upon $\{a^\dagger\}$. Under an orbital rotation $|\phi_0\rangle \rightarrow |\bar{\phi}_0\rangle = \exp(i\Lambda)|\phi_0\rangle$, the energy expectation value for a Hamiltonian H can be expanded in terms of $\{\Lambda_{rs}\}$ as

$$E(\{\Lambda_{rs}\}) = \langle\bar{\phi}_0|H|\bar{\phi}_0\rangle = \langle\phi_0|H|\phi_0\rangle - i\langle\phi_0|[\Lambda, H]|\phi_0\rangle - \frac{1}{2}\langle\phi_0|[\Lambda, [\Lambda, H]]|\phi_0\rangle + ... \tag{4}$$

When the optimal orbital basis for a given $\{C_g^{(0)}\}$ is used, the first derivative, $\langle\phi_0|[\Lambda, H]|\phi_0\rangle$, vanishes. In the component form, one requires

$$F_{rs} \equiv \langle\phi_0|[a_r^\dagger a_s, H]|\phi_0\rangle = 0 \tag{5}$$

for all (r, s) pairs. Eq. (5) is referred to as the generalized Brillouin condition. The orbital degree of freedom is thus described by Λ_{rs} $(r < s)$, and identifying the optimal orbitals amounts to finding $\{\Lambda_{rs}\}$ which minimizes the energy $E(\{\Lambda_{rs}\})$.

C. Orbital searching algorithm based on imaginary-time dynamics

The orbital equation of motion in real time is determined by finding the *single-particle* operator R that gives the best self-consistent approximation to the time evolution of the many-body state $|\phi\rangle$:

$$i\partial_t|\phi(t)\rangle \approx R|\phi(t)\rangle = \sum_{ij} R_{ij}a_i^\dagger a_j|\phi(t)\rangle \tag{6}$$

where $R_{ij} = \int dx \phi_i^*(x) i\partial_t \phi_j(x) = R_{ji}^*$. The Dirac-Frenkel time-dependent variational principle[21;23;24] is used to determine R, which gives

$$F_{rs} = \sum_k (D_{rk}R_{ks}^* - R_{rk}^*D_{ks}). \tag{7}$$

Note that F_{rs} [defined in Eq. (5)] and $D_{ij} = \langle\phi_0|a_i^\dagger a_j|\phi_0\rangle$ (the density matrix), are the two quantities needed to evaluate R. Once R is obtained, each orbital evolves according to $a_i^\dagger(t+dt) = a_i^\dagger(t) - i\sum_j R_{ji}a_j^\dagger(t)\,dt$. The derivation of Eq. (7) is given in the Appendix, and here we simply point out one property specific to the CAS scheme. The orbital rotations within "inactive" class or within "secondary" class do not affect the energy; the rotation within "active" class can also be ignored if we diagonalize the Hamiltonian in the CAS space. As a consequence, only rotations between orbitals of different classes matter (see the Appendix).

Our proposed orbital searching algorithm is based on the imaginary-time dynamics. Specifically at each orbital updating step $a_i^{(i)} = \sum_j X_{ij}a_j^{(i+1)}$, we *assign*

$$X = \exp(i\Lambda), \quad (i\Lambda)_{rs} = -(i\Lambda)_{sr}^* = R_{rs}\,d\tau, \quad r < s. \tag{8}$$

The order $r < s$ is important (see the discussion in Section III.A). $d\tau$ is a small number and its role will be discussed in Section III.B. The overall iteration procedure can now be summarized. One starts with a convenient orbital basis $\{a^{(0)}\}$ and diagonalizes H in Π-subspace to get $\{C^{(0)}\}$; Eq. (7) and Eq. (8) are then used to get $X^{(1)}$. These steps

are iterated as

$$\{a^{(0)}\} \rightarrow \{C^{(0)}\} \rightarrow a_i^{(0)} = \sum_j X_{ij}^{(1)} a_j^{(1)},$$

$$\{a^{(1)}\} \rightarrow \{C^{(1)}\} \rightarrow a_i^{(1)} = \sum_j X_{ij}^{(2)} a_j^{(2)},$$

$$\vdots \qquad (9)$$

$$\{a^{(n)}\} \rightarrow \{C^{(n)}\} \rightarrow a_i^{(n)} = \sum_j X_{ij}^{(n+1)} a_j^{(n+1)},$$

until $|F_{rs}|$ in Eq. (5) vanishes. Note that $a^{(0)} = X^{(1)} X^{(2)} ... X^{(n+1)} a^{(n+1)} \equiv U^{(n+1)} a^{(n+1)}$ and $U^{(n+1)} = U^{(n)} X^{(n+1)}$. The matrix $U^{(n)}$ relates $a^{(0)}$ and $a^{(n)}$, and is needed since the Hamiltonian is expressed in $a^{(0)}$ orbitals. Eqs. (7), (8) and (9) constitute the orbital searching algorithm.

III.   REMARKS ON THE ALGORITHM

A.   Basic idea and norm of a state

The basic idea behind this algorithm is simple: for a state propagating in imaginary time, the high-energy components decay exponentially. To be more explicit, we consider the time evolution of an arbitrary state $|\phi\rangle$,

$$|\phi(t)\rangle = \sum_n a_n e^{-iE_n t} |n\rangle$$

$$|\phi(-i\tau)\rangle = \sum_n a_n e^{-E_n \tau} |n\rangle, \qquad (10)$$

with $|n\rangle$ the exact eigenstates. One easily sees that by replacing $t \rightarrow -i\tau$, only the ground state component survives in the large τ limit.

The first practical issue is that the imaginary-time evolution does not conserve the norm of a state, so the orbital rotation based on the straightforward imaginary-time dynamics actually breaks the orthonormality of orbitals. There is no rigorous way to resolve this and the solution requires numerical testing. The mathematical conflict is that in Eq. (8), $(i\Lambda)$ is anti-Hermitian whereas R is Hermitian, therefore we can only assign half of the elements of R to $(i\Lambda)$. We find Eq. (8) (note the order $r < s$) works well for Hamiltonians of both real and complex coefficients. For real-coefficient Hamiltonians, we can use the Gram-Schmidt procedure proposed in Ref.[21] (see also the Appendix).

B.   Role of $d\tau$

There is a free parameter, $d\tau$ in Eq. (8), in the algorithm. The determination of its suitable values also requires numerical experiments. Generally, if $d\tau$ is small enough, the algorithm converges to the variational ground state. If the solution does converge, using larger $d\tau$ usually results in faster convergence [see Fig. 2 solid (black) and dashed (red) curves for illustration].

C.   Strategies to accelerate the convergence

We point out two general strategies, that can significantly accelerate the convergence. First, we should always start with calculations of a smaller CAS space and use the obtained orbital basis as the starting point for calculations

of a larger CAS space. Second, if using the Davidson algorithm to diagonalize the Hamiltonian, we should use the previously obtained ground state as the initial vector. Implementing these two strategies, one can accelerate the convergence by an order of magnitude.

D.   Comments on existing orbital searching algorithms

There are two existing orbital searching algorithms for CI-CAS calculations. The first algorithm uses the Newton-Raphson method or its variants to find the energy minimum in the orbital parameter space[25–27]. In this approach, at each iteration, the energy [see Eq. (4)] is minimized according to the quadratic expansion in orbital parameters $\{\Lambda_{rs}\}$. The convergence therefore depends critically on the starting orbital basis. Attempts beyond the Hessian (up to cubic order)[26,35] are reported to increase the stability, but are relatively time-consuming. Dealing with complex coefficients using these methods requires extra effort[25]. In Ref.[14], we proposed an orbital updating algorithm, which requires an additional RAS calculation. Our previous method is not sensitive to the starting orbital basis, but does not favor systems of many orbitals since the dimension of RAS grows polynomially as the orbital number increases. Overall, our previous approach does not take full advantage of the CAS scheme, whose dimension is independent of the total number of orbitals.

We note that direct imaginary-time dynamics is also used to obtain the CI variational ground state[21–23]. In this formalism, both orbitals ($\{a_i\}$) and states ($\{C_g\}$) evolve along the imaginary time, with a suitable wave-function normalization after every couple of time steps (as the norm is not conserved). A systematic study of this approach can be worthwhile (such as the initial orbital dependence and the spin-orbit coupling), and in principle, this method could have a comparable efficiency to ours. Here we simply point out that our proposed algorithm has a larger tolerance on the time step $d\tau$, and does not need to use a numerical method like Runge-Kutta for the time evolution, at the cost of updating $\{C_g\}$ by a matrix diagonalization instead of a matrix multiplication.

E.   Stability, efficiency, and complex-coefficient Hamiltonians

We conclude this section by emphasizing three distinct advantages of the proposed algorithm. First, it does not need a good starting orbital basis, and it converges to the ground state exponentially. When the initial state is too close too close to a local minimum (e.g. one of the excited states in the truncated space), the iteration converges to that state. However, as seen from Eq. (10), for a generic initial state that has non-negligible overlap with the ground state, the imaginary-time evolution leads to the ground state. The insensitivity to the starting orbital basis is a natural consequence of the imaginary-time dynamics. Second, as a minimization problem, the algorithm *only* needs the first derivative, which is the minimal requirement of any minimization procedure. As the Hessian is not required, it is time efficient and even the coding complexity is largely reduced. In essence, the proposed algorithm is the method steepest decent, which maximizes the overlap $|\langle \phi_{i+1}|e^{-d\tau \cdot H}|\phi_i\rangle|^2 \sim |\langle \phi_{i+1}|I - d\tau \cdot H|\phi_i\rangle|^2$ (with i and $i+1$ being two successive iterations), subject to the normalization of the state. Finally, the proposed algorithm does not distinguish real coefficients from complex, so the same formalism applies to Hamiltonians with complex coefficients[36], and this allows for investigating systems in which electron correlation and spin-orbit coupling are of comparable importance. Examples will be provided in the next section.

IV. SEVERAL ILLUSTRATIVE EXAMPLES

In this section we provide several illustrative examples to demonstrate the efficiency of the proposed algorithm. We solve impurity models[13] in which there are a few correlated orbitals coupled to several uncorrelated bath orbitals. Only the half-filled case, i.e. $N_o/2$ electrons occupying N_o spin-orbitals, is presented because it has the largest dimension for a given total orbital number. I   e algorithm.
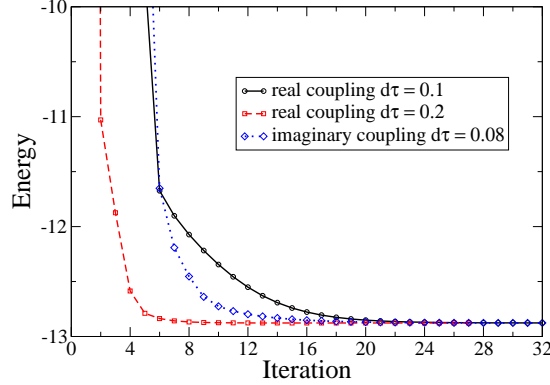

FIG. 2: (Color online) The convergence behavior of CAS(6,12) (total of 24 spin-orbitals) calculation for the three-orbital impurity model with Slater-Kanamori interaction. Black and red curves are using real hopping parameters; the red curve is using imaginary hopping parameter. Larger $d\tau$ leads to a faster convergence if the algorithm converges. They converge to the same energy as expected.

A. Zero and one spatial correlated orbital

We first apply our method to a non-interacting problem, and correlated problems using Hartree-Fock approximation (not shown). Recall that in the converged solution, the individual orbital depends on the initial orbital choice and may not respect the symmetry of the Hamiltonian, but that the resulting determinantal state built from these orbitals does. We next solve the single-site Anderson impurity model containing seven bath orbitals,

$$H = \varepsilon_d \sum_\sigma d_\sigma^\dagger d_\sigma + U n_{d,\uparrow} n_{d,\downarrow} + \sum_{p=2}^{8} \sum_\sigma t[d_\sigma^\dagger c_{p,\sigma} + h.c.] + \sum_{p=2}^{8} \sum_\sigma \varepsilon_p c_{p,\sigma}^\dagger c_{p,\sigma}. \tag{11}$$

We use d and c to denote the correlated and the bath orbitals, respectively. The parameters are fixed to be $\varepsilon_p = \pm 2, \pm 4/3, \pm 2/3, 0$, $t = 1/\sqrt{8}$, $U = 10$ and $\varepsilon_d = -U/2$. In Ref.[14] we have shown that only 36 determinantal states [within the CAS(4,8) subspace] are needed to faithfully describe the ground state. Using the proposed algorithm, the CAS(4,8) calculation practically finds the exact ground state with energy of -13.2465. When increasing the number of bath orbital to around 30[37], the current algorithm is at least two orders of magnitude faster (also using less computer memory) than our previous method[14].

B. Three correlated orbitals with Slater-Kanamori interaction

The Slater-Kanamori (SK) interaction plays an important role in systems where the conduction bands are mainly derived from the triply-degenerate t_{2g} orbitals of the transition metal[7,38]. A three-orbital impurity model with SK

interaction is given by

$$H_{3o} = H_{imp-SK} + H_{bath} + H_{imp-bath}, \tag{12}$$

where terms involving bath orbitals are

$$H_{bath} = \sum_{a=1}^{3} \sum_{i=1}^{N_b} \sum_{\sigma} \epsilon_i c_{ai,\sigma}^\dagger c_{ai,\sigma}$$

$$H_{imp-bath} = \sum_{a=1}^{3} \sum_{i=1}^{N_b} \sum_{\sigma} (t_i d_{a,\sigma}^\dagger c_{ai,\sigma} + H.c.). \tag{13}$$

Here N_b is the number of bath orbitals and σ labels the spin. The Slater-Kanamori term is

$$H_{imp-SK} = -\mu \sum_{a,\sigma} n_{a,\sigma} + U \sum_{a} n_{a,\uparrow} n_{a,\downarrow} + (U-2J) \sum_{a \neq b} n_{a,\uparrow} n_{b,\downarrow} + (U-3J) \sum_{a>b,\sigma} n_{a,\sigma} n_{b,\sigma}$$

$$+ J \sum_{a \neq b} (d_{a\uparrow}^\dagger d_{b\uparrow} d_{a\downarrow}^\dagger d_{b\downarrow} + d_{a\uparrow}^\dagger d_{b\uparrow} d_{b\downarrow}^\dagger d_{a\downarrow}), \tag{14}$$

with $a, b = 1, 2, 3$.

As an example we use $N_b = 3$, i.e. each (spatially) correlated orbital couples to three bath orbitals. A full CI calculation can be performed to obtain the exact result. We fix the parameters to be $\mu = -4$, $\epsilon_1 = -\epsilon_3 = -4/3$, $\epsilon_2 = 0$, $t_i = \sqrt{4 - \epsilon_i^2}/(2\pi)$, $U = 8$, $J = 1$. The exact ground state energy is -12.8831, and the CAS(6,12) calculation gives an energy of -12.8771, while CAS(8,16) gives an energy of -12.879. The convergence behavior of the CAS(6,12) calculation for $d\tau = 0.1, 0.2$ is shown in Fig. 2. As expected from the imaginary-time dynamics, an exponential convergence to the ground state energy is seen. The initial orbital basis is far from the solution, and leads to an initial energy around 50 that is beyond the presented scale[39]. The CAS(8,16) calculation only takes three iterations (not shown) to converge, when taking the results of CAS(6,12) as the starting point.

To test the algorithm involving complex coefficients, we assign each impurity-bath coupling with an extra phase factor, making it a complex number. In particular, the impurity-bath coupling becomes

$$H'_{imp-bath} = \sum_{a=1}^{3} \sum_{i=1}^{n_b} \sum_{\sigma} (e^{i\alpha_i} t_i d_{a,\sigma}^\dagger c_{ai,\sigma} + H.c.) \tag{15}$$

We note that by attaching a phase to each bath orbital $c_{ai,\sigma} \to e^{i\alpha_i} c_{ai,\sigma}$, Eq. (15) recovers Eq. (13), meaning these two Hamiltonians have the same ground state energy. In Fig. 2 (dotted curve in blue) we show the convergence of CAS(6,12) for $\alpha_i = \pi$, which is similar to what we obtained for real impurity-bath coupling. We have tested several phases ϕ_i and all of them converge to the same energy as they should (not shown).

C. Addition of spin-orbit coupling within correlated orbitals

Spin-orbit coupling is important for materials composed of heavier elements. For example, the spin-orbit-induced conduction band splitting at the Γ-point of $SrTiO_3$ ($3d$ material) is about 0.03 eV[40], whereas that of $KTaO_3$ ($5d$
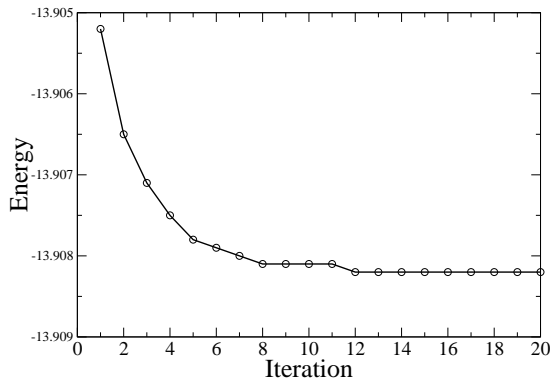
FIG. 3: The convergence behavior of CAS(6,12) (total of 24 spin-orbitals) calculation for the three-orbital impurity model with Slater-Kanamori and spin-orbit interaction.

material) is about 0.4 eV[30]. For three t_{2g} orbitals, the spin-orbit coupling can be expressed as[40–42]

$$
H_{so} = \Delta_{so} \begin{pmatrix}
0 & i & 0 & 0 & 0 & -1 \\
-i & 0 & 0 & 0 & 0 & i \\
0 & 0 & 0 & 1 & -i & 0 \\
0 & 0 & 1 & 0 & -i & 0 \\
0 & 0 & i & i & 0 & 0 \\
1 & -i & 0 & 0 & 0 & 0
\end{pmatrix},
\tag{16}
$$

where Δ_{so} parametrizes the couping strength. We note that the spin-orbit coupling breaks the spin SU(2) symmetry, and its complex coefficients cannot be made real by attaching a phase to each orbital. The convergence of the CAS(6,12) calculation, for $\Delta_{so} = 1$ [with all other parameters the same as those specified right below Eq. (14)] is shown in Fig. 3. If we use the orbital basis from the $\Delta_{so} = 0$ calculation as the starting point, the fast convergence is seen. The calculation converges to a ground state energy of -13.9082, whereas the full CI calculation gives -13.9144. In addition to the results presented here, we have tested the algorithm by increasing the number of bath (up to 50) and correlated orbitals (up to five), and in all cases we found the variational ground states without any difficulties.

D. Convergence and spectral function

	Exact	CAS(8,16)	CAS(6,12)	CI-4 CAS(6,12)	CAS(4,8)
$\Delta_{so} = 0$	-12.8831	-12.8790	-12.8771	-12.8770	-12.4040
$\Delta_{so} = 1$	-13.9144	-13.9113	-13.9082	-13.9077	-13.8607

TABLE I: Ground state energies obtained from different CI truncation schemes. The dimension of the CI space decreases from left to right. Calculation with larger CI subspace leads to a lower ground state energy.

Table I summarizes the ground state energies obtained with different CI schemes. As expected, including more states leads to a more accurate energy. If the exact solution is not available, the energy difference between CAS(6,12) and CAS(8,16), or between CAS(6,12) and CI-4 CAS(6,12), provides an error estimate of the CAS(6,12) result.

Another important and useful quantity is the spectral function or the impurity Green's function, the poles of which correspond to the *excitations* of the Hamiltonian. This quantity is essential in DMFT calculations and is
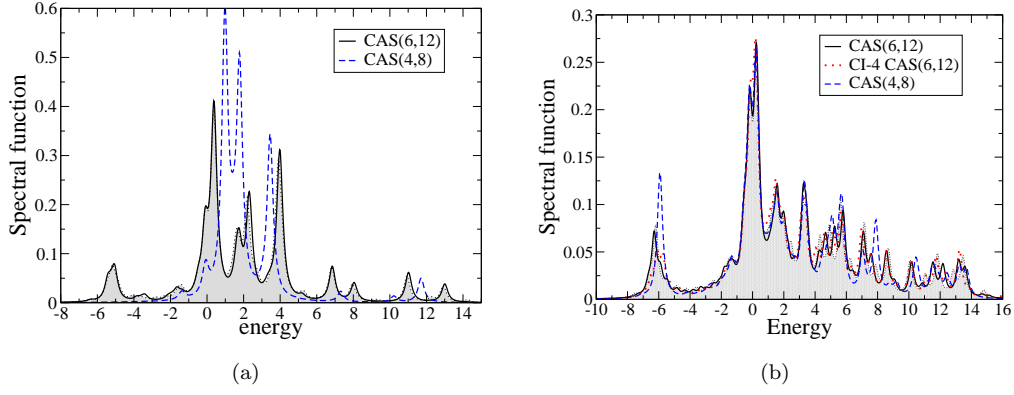
FIG. 4: (Color online) The spectral functions computed from different CI truncation schemes for a three-orbital impurity model with Slater-Kanamori interaction and different spin-orbit coupling strength Δ_{so}. A broadening of 0.2 is used and the full CI results are presented by dotted curves with shaded areas. (a) For $\Delta_{so} = 0$, the results from CAS(6,12) and CI-4 CAS(6,12) are almost identical so only the former is shown; the result from CAS(4,8) is significantly different from the exact one. (b) For $\Delta_{so} = 1$, the spectral functions using CAS(6,12), CI-4 CAS(6,12) and CAS(4,8) have qualitatively similar behavior.

directly related to photo-electron spectroscopic measurements. The steps to compute the spectral function are given in Ref.[14]. In Fig. 4(a) we show the spectral functions, projected on the first orbital, for $\Delta_{so} = 0$ using different CI schemes. Compared to the full CI result (dotted curves with shaded areas in Fig. 4), calculations using CAS(6,12) and CI-4 CAS(6,12) appear to be sufficient as the main features (i.e. peak positions and their relative weights) are well reproduced. The result using CAS(4,8) is very different from that using full CI, implying a significant portion of states is missed in this scheme. With spin-orbit coupling $\Delta_{so} = 1$, we find that all CAS(8,16), CAS(6,12), CI-4 CAS(6,12), and CAS(4,8) calculations give qualitatively similar spectral functions [Fig. 4(b)]. As there is no additional truncation involved in computing the spectral function, its accuracy depends only on the variational ground state, which can be characterized by its energy. Empirically, we find that when the energy difference between two CI calculations is smaller than 0.1, their spectral functions appear to be similar.

V. CONCLUSION

We establish an efficient and stable algorithm to identify the optimal single-particle basis by solving an equivalent multi-variable minimization problem. The algorithm is iterative and is based on imaginary-time dynamics. It improves the performance in at least three aspects. First, it requires only the first derivative but not the Hessian of the energy, which drastically reduces the time cost and the coding complexity. Second, the algorithm can converge even for almost random initial orbital basis choice, which is a consequence of imaginary-time dynamics. Finally, the algorithm can deal with Hamiltonians with complex coefficients without extra coding effort. We demonstrate the power of this method by applying it to several impurity problems, and explicitly compute the ground state energy and the spectral function to show the convergence of CI calculations. We expect our method to be valid in any system where CAS works well, and to be particularly useful for systems where electron correlation and spin-orbit coupling are both important and are of comparable strength.

Appendix A: Time-evolution of orbitals

1. General (real) time-dependence

We discuss the time-dependence based on the Refs.[21,23,24]. To find the equation of motion for the orbitals, we have to find the *single-particle* operator R that gives the best self-consistent approximation to the time evolution of the many-body state $|\phi\rangle$:

$$i\partial_t|\phi(t)\rangle \approx R|\phi(t)\rangle = \sum_{ij} R_{ij} a_i^\dagger a_j |\phi(t)\rangle$$

where $R_{ij} = \int dx \phi_i^*(x) i\partial_t \phi_j(x)$. Due to the orthonormality of orbital basis, i.e $\langle\phi_i(t)|\phi_j(t)\rangle = \delta_{ij}$, we get

$$R_{ij} = i\langle\phi_i|\partial_t\phi_j\rangle = -i\langle\partial_t\phi_i|\phi_j\rangle = (i\langle\phi_j|\partial_t\phi_i\rangle)^* = R_{ji}^*.$$

In other words, $R = R^\dagger$ is a Hermitian operator.

The equation for R is derived from the Dirac-Frenkel time-dependent variational principle, whose action S and its small variation are

$$
\begin{aligned}
S[\Psi] &= \int_0^T dt \langle\Psi|H - i\partial_t|\Psi\rangle, \\
\delta S &= \int_0^T dt \left[\langle\delta\Psi|H|\Psi\rangle + \langle\Psi|H|\delta\Psi\rangle - i\langle\delta\Psi|\dot\Psi\rangle + i\langle\dot\Psi|\delta\Psi\rangle \right] = 0.
\end{aligned}
\tag{A1}
$$

We have used $\langle\Psi|\delta\dot\Psi\rangle = -\langle\dot\Psi|\delta\Psi\rangle$. For a CI state $|\Psi\rangle = \sum_{g\in\Pi} |g\rangle C_g$ (Π specifies the CI space), a small variation can be described by

$$
\begin{aligned}
|\delta\Psi\rangle &= \sum_{g\in\Pi} |g\rangle\delta C_g + \Delta|\Psi\rangle \\
i|\dot\Psi\rangle &= i\sum_{g\in\Pi} |g\rangle\dot C_g + R|\Psi\rangle.
\end{aligned}
\tag{A2}
$$

Here Δ is an anti-hermitian [$\Delta_{ij} = -\Delta_{ji}^*$, also note that Δ is $i\Lambda$ in Eq. (2)]. The variation with respect to both δC_g and Δ_{ij} should vanish, from which we get

$$
\begin{aligned}
i\dot C_g &= \langle g|H - R|\Psi\rangle, \\
\langle\Psi|(H - R)(I - \Pi)a_i^\dagger a_j|\Psi\rangle &- \langle\Psi|a_i^\dagger a_j(I - \Pi)(H - R)|\Psi\rangle = 0
\end{aligned}
\tag{A3}
$$

The second equation of Eq. (A3) determines $R_{ij}(t)$.

2. Application to the CAS space

In the CAS approximation, the orbitals are grouped into "inactive" (I) (core), "active" (A), and "secondary" (S). For the orbital pairs (i, j) both belonging to the inactive or secondary class, $a_i^\dagger a_j |\Psi\rangle = 0$; for (i, j) both belonging to the active class, the projector $I - \Pi_{CAS}$ eliminates such contributions. Therefore, the pairs belonging to the same class are "redundant"[23]. For non-redundant pairs, the projector $I - \Pi_{CAS}$ has no effects and the equation for R, in component form, becomes

$$F_{rs} = \langle\Psi|[a_r^\dagger a_s, H]|\Psi\rangle = \sum_{ij}\langle\Psi|[a_r^\dagger a_s, R_{ij}a_i^\dagger a_j]|\Psi\rangle = \sum_k (R_{sk}D_{rk} - R_{kr}D_{ks})$$

$$= \sum_k (D_{rk}R_{ks}^* - R_{rk}^*D_{ks}) = (DR^* - R^*D)_{rs}. \tag{A4}$$

where $R_{ij} = R_{ji}^*$ is used. It is convenient to write D, R, and F in a block form, subject to the CAS constraints:

$$D = \begin{pmatrix} I & 0 & 0 \\ 0 & D_A & 0 \\ 0 & 0 & 0 \end{pmatrix}, \quad R = \begin{pmatrix} 0 & R_{IA} & R_{IS} \\ R_{IA}^\dagger & 0 & R_{AS} \\ R_{IS}^\dagger & R_{AS}^\dagger & 0 \end{pmatrix}, \quad F = \begin{pmatrix} 0 & F_{IA} & F_{IS} \\ -F_{IA}^\dagger & 0 & F_{AS} \\ -F_{IS}^\dagger & -F_{AS}^\dagger & 0 \end{pmatrix}. \tag{A5}$$

By expressing $DR^* - R^*D$ also in a block form, we obtain $R_{IS}^* = F_{IS}$, $R_{AS}^* = D_A^{-1}F_{AS}$, $R_{IA}^* = F_{IA}(I - D_A)^{-1}$. To get the transformation of single-particle orbitals, one first note that $i\partial_t|\phi(t)\rangle \approx \sum_{ij} R_{ij}a_i^\dagger(t)a_j(t)|\phi(t)\rangle$, which implies

$$|\phi(t + dt)\rangle \approx |\phi(t)\rangle - iR\,dt\,|\phi(t)\rangle \tag{A6}$$

We choose $|\phi(t)\rangle = a_k^\dagger(t)|0\rangle$ with $|0\rangle$ being the no-particle vacuum state, and write $|\phi(t + dt)\rangle = a_k^\dagger(t + dt)|0\rangle$, we get

$$|\phi(t + dt)\rangle = a_k^\dagger(t)|0\rangle - i\,dt \sum_{ij} R_{ij}a_i^\dagger(t)a_j(t)a_k^\dagger(t)|0\rangle$$

$$= \left[a_k^\dagger(t) - i\,dt \sum_i R_{ik}a_i^\dagger(t) \right]|0\rangle \equiv a_k^\dagger(t + dt)|0\rangle. \tag{A7}$$

We end up with the transformation

$$a_k^\dagger(t + dt) = \sum_i a_i^\dagger(t)(\delta_{ik} - i\sum_j R_{ik}\,dt) \approx \sum_i a_i^\dagger(t)\,[\exp(-iR\,dt)]_{ik}. \tag{A8}$$

3. Imaginary time

For the imaginary-time dynamics, one replaces $it \to \tau$, or $t \to -i\tau$. In this case, Eq. (A8) becomes $a_i^\dagger(\tau + d\tau) = a_i^\dagger(\tau) - \sum_j R_{ji}a_j^\dagger(\tau)d\tau \equiv \sum_j a_j^\dagger(\tau)A_{ji}$. As discussed in Section III.A, A is not unitary. Following Ref.[21], we can use Gram-Schmidt procedure to construct a unitary matrix. The simplest way is to use QR-decomposition, i.e. decomposing A into $A = QR$ with Q a unitary matrix and R an upper triangular matrix. In the present work, we use Eq. (8) to extract a unitary matrix from A.

---

[1] T. Helgaker, P. Jørgensen, and J. Olsen, *Molecular Electronic-Structure Theory* (Job Wiley & Sons, LTD., 2000).

[2] C. D. Sherrill and H. F. Schaefer III, *in The Configuration Interaction Method: Advances in Highly Correlated Approaches, Advances in Quantum Chemistry, Vol. 34,* (edited by P. O. Lowdin, J. R. Sabin, M. C. Zerner, and E. Brandas, Academic, New York, pp. 143-269, 1999).

[3] K. G. Wilson, Rev. Mod. Phys. **47**, 773 (1975), URL http://link.aps.org/doi/10.1103/RevModPhys.47.773.

[4] J. R. Schrieffer and P. A. Wolff, Phys. Rev. **149**, 491 (1966), URL http://link.aps.org/doi/10.1103/PhysRev.149.491.

[5] A. C. Hewson, *The Kondo Problem to Heavy Fermion* (Cambridge University Press, 1993).

[6] E. Dagotto, Rev. Mod. Phys. **66**, 763 (1994).

[7] M. Imada, A. Fujimori, and Y. Tokura, Rev. Mod. Phys. **70**, 1039 (1998), URL http://link.aps.org/doi/10.1103/RevModPhys.70.1039.

[8] H. v. Löhneysen, A. Rosch, M. Vojta, and P. Wölfle, Rev. Mod. Phys. **79**, 1015 (2007), URL http://link.aps.org/doi/10.1103/RevModPhys.79.1015.

[9] S. Blügel, Phys. Rev. Lett. **68**, 851 (1992), URL http://link.aps.org/doi/10.1103/PhysRevLett.68.851.

[10] D. E. Woon and T. H. Dunning Jr, J. Chem. Phys. **99**, 1914 (1993).

[11] D. Zgid and G. K.-L. Chan, J. Chem. Phys. **134**, 094115 (2011).

[12] D. Zgid, E. Gull, and G. K.-L. Chan, Phys. Rev. B **86**, 165128 (2012).

[13] O. Gunnarsson and K. Schönhammer, Phys. Rev. B **28**, 4315 (1983), URL http://link.aps.org/doi/10.1103/PhysRevB.28.4315.

[14] C. Lin and A. A. Demkov, Phys. Rev. B **88**, 035123 (2013), URL http://link.aps.org/doi/10.1103/PhysRevB.88.035123.

[15] A. Go and A. Millis, *Spatial correlations and the insulating phase of the high-tc cuprates: insights from a configuration interaction based solver for dynamical mean field theory*, arXiv:1311.6819.

[16] A. Georges, G. Kotliar, W. Krauth, and M. J. Rozenberg, Rev. Mod. Phys. **68**, 13 (1996).

[17] T. Maier, M. Jarrell, T. Pruschke, and M. H. Hettler, Rev. Mod. Phys. **77**, 1027 (2005).

[18] G. Kotliar and D. Vollhardt, Physics Today **57** (2004).

[19] G. Kotliar, S. Y. Savrasov, K. Haule, V. S. Oudovenko, O. Parcollet, and C. A. Marianetti, Rev. Mod. Phys. **78**, 865 (2006).

[20] E. Gull, A. J. Millis, A. I. Lichtenstein, A. N. Rubtsov, M. Troyer, and P. Werner, Rev. Mod. Phys. **83**, 349 (2011), URL http://link.aps.org/doi/10.1103/RevModPhys.83.349.

[21] T. Kato and H. Kono, Chem. Phys. Lett. **392**, 533 (2004).

[22] M. Nest, T. Klamroth, and P. Saalfrank, J. Chem. Phys. **122**, 124102 (2005).

[23] T. Sato and K. L. Ishikawa, Phys. Rev. A **88**, 023402 (2013), URL http://link.aps.org/doi/10.1103/PhysRevA.88.023402.

[24] R. P. Miranda, A. Fisher, L. Stella, and A. P. Horsfield, J. Chem. Phys. **134**, 244101 (2011).

[25] E. Dalgaard and P. Jørgensen, J. Chem. Phys. **69(8)**, 3833 (1978).

[26] J. Olsen, D. L. Yeager, and P. Jørgensen, *Advances in Chemical Physics, Vol.54* (edited by I. Prigogine and Stuard A. Rice, John Wiley & Son, pp. 1-176, 1983).

[27] H. Werner and P. J. Knowles, J. Chem. Phys. **82 (11)**, 5053 (1985).

[28] H. Werner and P. J. Knowles, J. Chem. Phys. **89**, 5803 (1988).

[29] D. L. Yeager, P. Albertson, and P. Jørgensen, J. Chem. Phys. **73(6)**, 2811 (1980).

[30] H. Nakamura and T. Kimura, Phys. Rev. B **80**, 121308 (2009), URL http://link.aps.org/doi/10.1103/PhysRevB.80.121308.

[31] B. J. Kim, H. Jin, S. J. Moon, J.-Y. Kim, B.-G. Park, C. S. Leem, J. Yu, T. W. Noh, C. Kim, S.-J. Oh, et al., Phys. Rev. Lett. **101**, 076402 (2008), URL http://link.aps.org/doi/10.1103/PhysRevLett.101.076402.

[32] A. Shitade, H. Katsura, J. Kuneš, X.-L. Qi, S.-C. Zhang, and N. Nagaosa, Phys. Rev. Lett. **102**, 256403 (2009), URL http://link.aps.org/doi/10.1103/PhysRevLett.102.256403.

[33] E. R. Davidson, Journal of Computational Physics **17**, 87 (1975), ISSN 0021-9991.

[34] Certainly when the CI space is small enough, the dense matrix algorithm should be used.

[35] J. Olsen, P. Jørgensen, and D. L. Yeager, J. Chem. Phys. **77**, 356 (1982).

[36] Practically this means that the code written for real-coefficient Hamiltonians can be applied to complex-coefficient Hamiltinians, by simply replacing all real variables by complex ones.

[37] C. Lin and A. A. Demkov, Phys. Rev. Lett. **111**, 217601 (2013), URL http://link.aps.org/doi/10.1103/PhysRevLett.

111.217601.

[38] P. Werner, E. Gull, and A. J. Millis, Phys. Rev. B **79**, 115119 (2009), URL `http://link.aps.org/doi/10.1103/PhysRevB.79.115119`.

[39] Here the initial orbitals are chosen to diagonalize the single-particle Hamiltonian. We also purposely use several initial orbital bases which are far away from the solution, and they all converge to the variational ground state.

[40] Z. Zhong, A. Tóth, and K. Held, Phys. Rev. B **87**, 161102 (2013), URL `http://link.aps.org/doi/10.1103/PhysRevB.87.161102`.

[41] G. Khalsa and A. H. MacDonald, Phys. Rev. B **86**, 125121 (2012), URL `http://link.aps.org/doi/10.1103/PhysRevB.86.125121`.

[42] Z. Zhong, Q. Zhang, and K. Held, Phys. Rev. B **88**, 125401 (2013), URL `http://link.aps.org/doi/10.1103/PhysRevB.88.125401`.